Crystal structures and compressibilities of pyrope and grossular to 60 kbar

ROBERT M. HAZEN AND LARRY W. FINGER

Geophysical Laboratory, Carnegie Institution of Washington
Washington, D. C. 20008

Abstract

Crystal structures and compressibilities of the end-member garnets pyrope (synthetic $Mg_3Al_2Si_3O_{12}$ at 1 bar and 16, 31, 43, and 56 kbar) and grossular (natural $Ca_3Al_2Si_3O_{12}$ at 1 bar and 19, 35, and 61 kbar) have been determined from three-dimensional, single-crystal X-ray data. Both garnets have cubic unit-cell dimensions within experimental error: for pyrope $a = 11.456(1)$A at 1 bar and 11.332(5)A at 50 kbar; for grossular $a = 11.846(1)$A at 1 bar and 11.720(5)A at 50 kbar. Bulk moduli of pyrope and grossular are both approximately 1350(50) kbar, which agrees with previous static compression data but is significantly lower than elastic constant data.

The large, eight-coordinated polyhedra compress more than the aluminum octahedra, which compress more than the silicon tetrahedra. Polyhedral bulk moduli are 1150(125), 1300(100), 2200(500), and 3000(1000) kbar, respectively, for $^{VIII}Ca^{2+}$, $^{VIII}Mg^{2+}$, $^{VI}Al^{3+}$, and $^{IV}Si^{4+}$. The observed compression of the silicon tetrahedron is significantly greater than previously reported experimental or theoretical values. In the eight-coordinated site, linear compression of four longer M–O bonds is approximately twice that of four shorter bonds. Thus, this polyhedron becomes more regular at high pressure.

Introduction

Garnets are assumed to be important mantle silicate minerals, on the basis of their common occurrence in garnet peridotites and eclogites and their experimentally determined high-pressure stability fields. Consequently, the variations of the structure and physical properties of garnet with pressure are important in formulating and constraining models of the earth's interior. The principal objectives of this study were:

(1) to determine the compressibilities and crystal structures of pyrope and grossular as a function of pressure,

(2) to compare these results with known high-temperature variations of garnet structure (Meagher, 1975), and

(3) to compare these results with predictions of structural changes at high pressure by Hazen and Prewitt (1977).

The crystal structures and thermal expansion of pyrope and grossular at several temperatures to 750°C were reported by Meagher (1975), who cited previous studies of garnet structure. Recent investigations of garnet compressibility include elastic con-

stant data on pyrope–almandine by Anderson *et al.* (1968), static compression on a garnet of unreported composition by Vaidya *et al.* (1973), shock-wave data on almandine to 650 kbar by Graham and Ahrens (1973), and elastic-constant measurements on pyrope to 10 kbar by Bonczar *et al.* (1977). Details of the garnet crystal structure at high pressure have been predicted by Huggins (1974), but no previous high-pressure structural determinations have been published.

Experimental

Specimen description

Single crystals of pure synthetic pyrope ($Mg_3Al_2Si_3O_{12}$) were kindly provided by Professor E. P. Meagher from material originally synthesized by Dr. F. R. Boyd, Geophysical Laboratory. Conditions of synthesis were 1300°C and 36 kbar in the presence of water. The room-pressure unit-cell edge, $a = 11.456 \pm 0.001$A, agrees with previous studies of this material (Gibbs and Smith, 1965; Meagher, 1975).

Colorless euhedral crystals of a natural end-mem-

ber grossular ($Ca_3Al_2Si_3O_{12}$, with 0.5 weight percent FeO) were kindly supplied by Professor Clifford Frondel (Harvard Mineralogical Museum No. 95454). The unit-cell edge of this specimen from Georgetown, California, is $a = 11.846 \pm 0.001$A, which agrees with the cell edge determined by Pabst (Yoder, 1950) for this material. This value is also identical with that reported by Meagher (1975) for the unit cell of natural grossular from Asbestos, Quebec.

High-pressure techniques

Garnet single crystals, approximately 100 μm in maximum dimension and no greater than 50 μm thick, were mounted in a diamond-anvil high-pressure cell (Merrill and Bassett, 1974) using Inconel 750X (International Nickel Company, Inc.) gaskets, and water + glycerin as the hydrostatic pressure medium. Ruby crystals 10 μm in size were included in the mount, and pressures were calibrated to ± 1 kbar using the pressure shift of the R_1 ruby fluorescence line (Piermarini et al., 1975). At each pressure, the pressure and unit-cell dimensions were measured, X-ray intensity data were collected, and the pressure and unit-cell dimensions were remeasured. In all instances the pressures and unit-cell dimensions measured before data collection agreed within experimental error with the values determined after data collection. Thus, no relaxation of the pressure cell was observed to 60 kbar.

Details of procedures for crystal mounting, crystal centering on the four-circle diffractometer, unit-cell determination, and data collection are described elsewhere (Hazen, 1976a; Finger and King, 1978).

Data collection and refinement

Intensity measurements were made on an automated four-circle Picker diffractometer with Nb-filtered, MoKα radiation, using the constant precision intensity technique described by Finger et al. (1973) and the fixed-ϕ mode of data collection at high pressure (Finger and King, 1978). All reflections in one octant of reciprocal space from 0.1 to 0.9 sin θ/λ were collected at room pressure, and all accessible reflections in one hemisphere of reciprocal space from 0.1 to 0.7 sin θ/λ were collected at high pressure. The number of independent observed reflections ($I > 2\sigma$), R values, and unit-cell parameters are listed in Table 1

The observed intensities were corrected for absorption ($\mu_l = 11.8$ and 26.5 cm^{-1} for pyrope and grossular, respectively), and refinement was accomplished using program RFINE (Finger and Prince, 1975).[1] Neutral scattering factors of Cromer and Mann (1968) and coefficients for anomalous scattering of Cromer and Liberman (1970) were used for all atoms.

The garnet structure has four atoms in the asymmetric unit; the three metal atoms are in special positions with all atomic coordinates constrained ($^{VIII}R^{2+}$ at 1/8, 0, 1/4; Al at 0, 0, 0; Si at 3/8, 0, 1/4), whereas the oxygen is in the general position. Room-pressure intensity data were refined using a model with anisotropic temperature factors and constraints described by Gibbs and Smith (1965). High-pressure refinements were not significantly improved using anisotropic temperature factors [as determined by Hamilton's (1965) significance test], and isotropic temperature factors were thus used in those refinements.

The number of reflections in the high-pressure experiments is greatly reduced from a 1 bar data set because of the limited region of reciprocal space that is accessible, and because of the unfavorable peak-to-background ratios. For high-symmetry materials, atoms in special positions have nonspace-group absence conditions that reduce the number of data for which these atoms have nonzero contributions. In garnet the silicon and eight-coordinated atoms have identical special-absence conditions; therefore, refinement of the thermal parameters for these positions is based on the same small set of observations. In the refinement of the high-pressure data the resulting correlation coefficient between the temperature factors for these atoms is approximately -0.96, and independent refinement is impossible. It was necessary, therefore, to constrain the ratio of these factors to the value observed at room pressure. Refined oxygen atomic coordinates and isotropic temperature factors are given in Table 2. Room-pressure anisotropic temperature coefficients are in agreement with those of Meagher (1975) and are not republished here.

Results

Garnet bulk moduli

Least-squares fit of unit-cell volume (A^3) vs. pressure (kbar) to a quadratic equation yields

---

[1] Tabulated observed and calculated structure factors are available from the authors on request. (N.B.: the published structure factors of Meagher (1975), Table 4, are apparently calculated for the content of a primitive cell and should be multiplied by a factor of two for the body-centered cell; i.e., F_o of (400) should read 400.6 instead of 200.3)

Table 1. Garnet refinement conditions and unit-cell parameters

P (kbar)	a (Å)	No. of independent observed reflections	R (%)*	Weighted R (%)**
		Pyrope		
1 bar	11.456(1)†	212	3.9	3.0
16(1)	11.412(4)	40	4.9	1.7
31(1)	11.377(4)	43	4.4	1.4
43(1)	11.352(5)	39	4.0	1.6
56(1)	11.318(5)	34	4.5	1.2
		Grossular		
1 bar	11.846(1)	318	3.6	1.5
19(1)	11.795(4)	90	3.9	1.6
35(1)	11.760(4)	87	4.8	2.6
61(1)	11.698(4)	42	11.3	6.8

*$R = \Sigma||F_o| - |F_c||/\Sigma|F_o|$.
**Weighted $R = [\Sigma w(|F_o| - |F_c|)^2/\Sigma wF_o^2]^{1/2}$.
†Parenthesized figures represent esd's of least units cited.

$$V_{\text{pyrope}} = 1503.5(1) - 1.13(2)P + 0.004(1)P^2,$$

and

$$V_{\text{grossular}} = 1662.3(1) - 1.20(4)P + 0.005(1)P^2.$$

The room-pressure bulk moduli are 1330(30) and 1390(50) kbar, respectively, for pyrope and grossular. These values are in agreement with the 1375 kbar bulk modulus determined by Vaidya et al. (1973), using static compression to 45 kbar on a garnet of unspecified composition. These values are significantly smaller, however, than the 1650 to 1770 kbar bulk moduli of silicate garnets recorded by several investigators using elastic constant data (Verma, 1960; Anderson et al., 1968; Bonczar et al., 1977).

The magnitude of this discrepancy is illustrated in Figure 1, which is a plot of V/V_0 vs. pressure for the pyrope and grossular of this study, as well as the natural pyrope (with 36 atom percent Fe in the eight-coordinated site) studied by Bonczar et al. (1977). It is not clear why bulk moduli determined by elastic-constant measurements should be consistently higher than those determined at static pressure for these garnets.

The silicon tetrahedron

Selected interatomic distances and angles are presented in Tables 3 and 4. The format used is identical with that of Meagher (1975) for ease of comparison. Polyhedral volumes and distortion indices (Robinson et al., 1971) are listed in Table 5. Silicon–oxygen interatomic distances, as well as silicon tetrahedral volumes, show small but statistically significant decreases with increasing pressure. In both garnets the distances decrease by four standard errors (±0.012Å) at 60 kbar, on the basis of linear regression analysis of distance vs. pressure data. Mean linear compressibilities of Si–O bonds are approximately $110 \pm 40 \times 10^{-6}$ kbar^{-1} for both pyrope and grossular, and polyhedral bulk moduli for the silicon tetrahedra are 3000 ± 1000 kbar. It should be noted that these values represent changes in bond distance of approximately 0.5 percent at 50 kbar, and compressibilities and bulk moduli are therefore subject to large errors.

The observed compression of tetrahedral Si–O bonds, and consequent tetrahedral compressibility, are larger than previously reported experimental or

Table 2. Garnet positional parameters and isotropic temperature factors at several pressures

P (kbar)	Oxygen X	Oxygen Y	Oxygen Z	B_{Si}	B_{Al}	$B_{Mg,Ca}$	B_O
			Pyrope				
1 bar	0.0328(2)*	0.0502(2)	0.6534(2)	0.32(3)	0.31(3)	0.70(5)	0.35(3)
16(1)	0.0329(4)	0.0495(4)	0.6532(4)	0.32(4)	0.44(10)	0.73(9)	0.24(18)
31(1)	0.0327(3)	0.0503(3)	0.6522(3)	0.3(1)	0.5(1)	0.69(8)	0.2(2)
43(1)	0.0331(4)	0.0503(3)	0.6532(4)	0.3(1)	0.2(1)	0.78(8)	0.5(2)
56(1)	0.0313(3)	0.0506(4)	0.6535(4)	0.3(1)	0.0(1)	0.6(1)	0.9(2)
			Grossular				
1 bar	0.0380(1)	0.0450(1)	0.6518(1)	0.29(4)	0.25(1)	0.33(2)	0.35(2)
19(1)	0.0372(3)	0.0458(3)	0.6516(3)	0.3(1)	0.45(4)	0.6(1)	0.5(1)
35(1)	0.0379(3)	0.0458(4)	0.6518(3)	0.3(2)	0.5(1)	0.7(2)	0.5(1)
61(1)	0.0359(18)	0.0414(17)	0.6496(24)	0.4(1)	0.5(4)	0.9(2)	0.4(4)

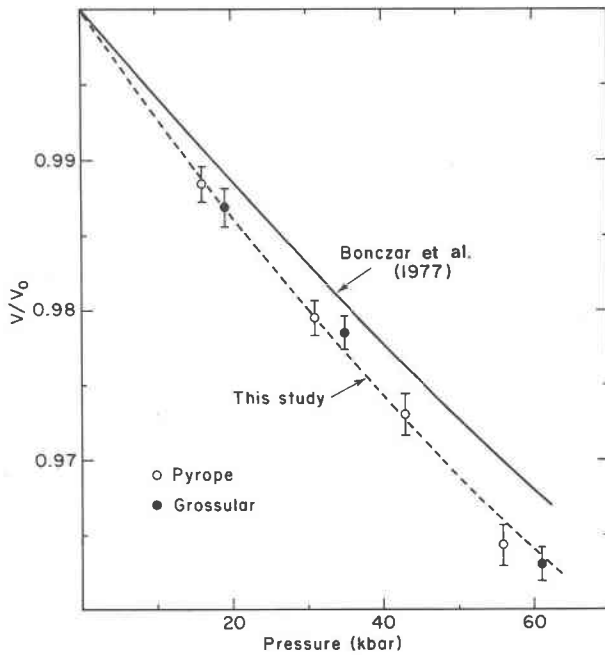*Parenthesized figures represent esd's of least units cited.

Fig. 1. V/V_0 vs. pressure for pyrope and grossular. Elastic constant data of Bonczar *et al.* (1977) on a natural pyrope are presented for comparison.

theoretical values. Huggins (1974) predicted a value of 14,000 kbar for the bulk modulus of silicon tetrahedra in andradite. Hazen (1976b) observed no Si–O compression within experimental error in forsterite, and Hazen and Prewitt (1977) suggested a silicon tetrahedral bulk modulus of 8000 kbar, on the basis

of their empirical compression equation. On the other hand, the 3000 ± 1000 kbar tetrahedral bulk moduli of garnets are close to the 2500 ± 1500 kbar values recently measured for silicon tetrahedra in the spinel forms of Ni_2SiO_4 and Fe_2SiO_4 (Finger and Hazen, 1977a). Studies now in progress on high-pressure crystal structures of clinopyroxenes, layer silicates, and quartz will provide additional data on the behavior of silicon–oxygen bonds under pressure.

The aluminum octahedron

Aluminum–oxygen bonds show significant shortening between room pressure and 60 kbar. In both garnets the mean Al–O linear compressibilities are approximately $190 ± 30 × 10^{-6}$ $kbar^{-1}$, and octahedral bulk moduli are 2200 ± 500 kbar. Thus, Al–O bonds shorten by approximately 1.0 percent at 50 kbar. These values are similar to the Al–O linear compressibility of $150 × 10^{-6}$ $kbar^{-1}$ and the octahedral bulk modulus of 2300 kbar observed for ruby corundum (Finger and Hazen, 1977b), but are considerably different from the linear compressibility of $100 × 10^{-6}$ $kbar^{-1}$ and the bulk modulus of 4000 kbar predicted by Hazen and Prewitt (1977).

As noted by Meagher (1975), the aluminum octahedral site is nearly regular, with distortion indices only slightly greater than their ideal values (see Table 5). Octahedral distortions do not change appreciably with pressure, and therefore the site remains regular at high pressure.

Table 3. Selected interatomic distances (Å)

Pyrope		1 bar	16 kbar	31 kbar	43 kbar	56 kbar	Grossular		1 bar	19 kbar	35 kbar	61 kbar
Si–O	[4]*	1.634(2)†	1.626(4)	1.633(3)	1.619(4)	1.626(3)	Si–O	[4]	1.643(1)	1.646(4)	1.635(4)	1.64(2)
O(1)–O(2)	[2]	2.495(4)	2.481(9)	2.502(7)	2.476(9)	2.465(8)	O(1)–O(2)	[2]	2.560(3)	2.560(8)	2.548(9)	2.54(5)
O(1)–O(3)	[4]	2.751(4)	2.738(7)	2.745(6)	2.724(7)	2.746(6)	O(1)–O(3)	[4]	2.743(3)	2.750(6)	2.728(6)]	2.67(4)
Mean O–O		2.665	2.610	2.624	2.600	2.606	Mean O–O		2.652	2.655	2.638	2.61
Al–O	[6]	1.887(2)	1.875(5)	1.862(4)	1.869(5)	1.863(5)	Al–O	[6]	1.929(1)	1.919(4)	1.918(4)	1.86(3)
O(1)–O(4)	[6]	2.618(4)	2.607(7)	2.582(6)	2.595(7)	2.567(6)	O(1)–O(4)	[6]	2.694(3)	2.693(6)	2.685(7)	2.60(4)
O(1)–O(5)	[6]	2.717(4)	2.696(9)	2.683(8)	2.690(9)	2.702(8)	O(1)–O(5)	[6]	2.761(3)	2.735(6)	2.739(6)	2.67(4)
Mean O–O		2.668	2.652	2.633	2.643	2.620	Mean O–O		2.728	2.721	2.712	2.64
Mg(1)–O(4)	[4]	2.197(2)	2.188(5)	2.188(4)	2.180(5)	2.156(4)	Ca(1)–O(4)	[4]	2.317(2)	2.302(4)	2.301(4)	2.27(2)
Mg(2)–O(4)	[4]	2.343(2)	2.341(4)	2.323(4)	2.320(4)	2.307(4)	Ca(2)–O(4)	[4]	2.490(2)	2.468(4)	2.462(4)	2.49(2)
Mean Mg–O		2.270	2.270	2.270	2.256	2.234	Mean Ca–O		2.404	2.384	2.381	2.38
O(1)–O(2)	[2]	2.495(4)	2.481(9)	2.502(7)	2.476(9)	2.465(8)	O(1)–O(2)	[2]	2.560(3)	2.560(8)	2.548(9)	2.54(5)
O(1)–O(4)	[4]	2.618(4)	2.607(7)	2.582(6)	2.595(7)	2.567(6)	O(1)–O(4)	[4]	2.761(3)	2.735(6)	2.739(6)	2.67(4)
O(4)–O(6)	[4]	2.709(4)	2.712(10)	2.702(9)	2.688(9)	2.649(9)	O(4)–O(6)	[4]	2.967(3)	2.934(7)	2.931(8)	2.91(5)
O(1)–O(7)	[4]	3.307(2)	3.296(4)	3.293(3)	3.279(4)	3.262(4)	O(1)–O(7)	[4]	3.448(1)	3.431(3)	3.421(3)	3.42(2)
O(4)–O(7)	[2]	2.782(4)	2.780(9)	2.757(7)	2.751(8)	2.746(6)	O(4)–O(7)	[2]	2.868(3)	2.854(8)	2.836(9)	2.75(4)
O(7)–O(8)	[2]	3.825(4)	3.822(8)	3.791(7)	3.753(5)	3.759(5)	O(7)–O(8)	[2]	4.120(3)	4.076(7)	4.075(8)	4.08(4)
Mean O–O		2.930	2.923	2.912	2.889	2.881	Mean O–O		3.099	3.076	3.071	3.04
Mean O–O cube		2.655	2.650	2.638	2.616	2.608	Mean O–O cube		2.813	2.792	2.787	2.74

*Bracketed figures represent bond multiplicities.
†Parenthesized figures represent *esd*'s of least units cited.

Table 4. Selected interatomic angles (degrees)

Pyrope		1 bar	16 kbar	31 kbar	43 kbar	56 kbar	Grossular		1 bar	19 kbar	35 kbar	61 kbar
O(1)-Si-O(2)	[2]*	99.5(1)†	99.5(2)	100.0(3)	99.8(3)	98.6(3)	O(1)-Si-O(2)	[2]	102.4(1)	102.1(3)	102.4(3)	101.8(9)
O(1)-Si-O(3)	[4]	114.7(1)	114.7(2)	114.4(2)	114.5(2)	115.2(2)	O(1)-Si-O(3)	[4]	113.1(1)	113.3(2)	113.1(2)	113.7(9)
O(1)-Al-O(4)	[6]	87.9(1)	88.1(2)	87.8(2)	88.0(2)	87.1(2)	O(1)-Al-O(4)	[6]	88.6(1)	89.1(1)	88.8(2)	88.5(8)
O(1)-Al-O(5)	[6]	92.1(1)	91.3(2)	92.2(2)	92.0(2)	92.9(2)	O(1)-Al-O(5)	[6]	91.4(1)	90.9(1)	91.2(2)	91.5(8)
O(1)-Mg-O(2)	[2]	69.2(1)	69.1(2)	69.8(2)	69.2(2)	69.8(2)	O(1)-Ca-O(2)	[2]	67.1(1)	67.6(2)	67.2(2)	68(1)
O(1)-Mg-O(4)	[4]	70.4(1)	70.2(2)	69.8(2)	70.4(2)	70.1(2)	O(1)-Ca-O(4)	[4]	70.0(1)	69.9(2)	70.1(2)	68(1)
O(4)-Mg-O(6)	[4]	73.2(1)	73.5(2)	73.5(2)	73.3(2)	73.7(2)	O(4)-Ca-O(6)	[4]	70.3(1)	70.7(2)	70.3(2)	71(1)
O(4)-Mg-O(7)	[2]	72.9(1)	72.9(2)	72.8(2)	72.7(2)	72.7(2)	O(4)-Ca-O(7)	[2]	76.1(1)	75.8(1)	75.9(1)	77(1)
O(1)-Mg-O(7)	[4]	93.5(1)	93.3(1)	93.7(1)	93.5(1)	93.9(1)	O(1)-Ca-O(7)	[4]	91.6(1)	91.9(1)	91.8(1)	92(1)
O(7)-Mg-O(8)	[2]	109.5(1)	109.4(2)	109.4(2)	109.6(2)	108.6(2)	O(7)-Ca-O(8)	[2]	111.7(1)	111.3(2)	111.7(2)	110(1)

*Bracketed figures represent multiplicities of bonds.
†Parenthesized figures represent *esd*'s of least units cited.

The eight-coordinated site

In both garnets the large eight-coordinated site is the most compressible polyhedron. In pyrope, magnesium–oxygen bonds compress at an average rate of $270 \pm 20 \times 10^{-6}$ kbar^{-1}, and the bulk modulus of the polyhedron is 1300 ± 100 kbar. In grossular, calcium–oxygen mean linear compression is $290 \pm 25 \times 10^{-6}$ kbar^{-1}, and the bulk modulus is 1150 ± 125 kbar. In both pyrope and grossular, therefore, the mean M–O distance in the eight-coordinated site compresses by 1.5 percent at 50 kbar. As in the silicon tetrahedron and aluminum octahedron, this site displays greater compressibility than that predicted by the empirical equation of Hazen and Prewitt (1977), which suggests values of 220 and 230×10^{-6} kbar^{-1}, respectively, for mean linear Mg–O and Ca–O compression.

Four shorter $M(1)$–$O(4)$ and four longer $M(2)$–$O(4)$ bonds are found in each eight-coordinated site. In both garnets studied the longer bonds compress significantly more than the shorter bonds, tending to make this polyhedron more regular at higher pressure.

Comparison of structural changes as a function of temperature, pressure, and composition

Hazen and Prewitt (1977) have noted that an "inverse relationship" exists between structural changes with temperature and pressure in several silicate mineral groups, including olivines and alkali feldspars. In these minerals, changes of crystal structure on cooling from high temperature are similar to changes on compression. Pyrope displays the inverse relationship to a first approximation. With both cooling and compression, the silicon tetrahedron is the most rigid structural element, showing little change in size or

Table 5. Garnet polyhedral volumes (A³) and distortion indices

Polyhedron	Pyrope					Grossular			
	1 bar	16 kbar	31 kbar	43 kbar	56 kbar	1 bar	19 kbar	35 kbar	61 kbar
Si tetrahedron									
Volume	2.19	2.15	2.19	2.13	2.15	2.25	2.26	2.22	2.24
Quadratic elongation	1.015	1.015	1.014	1.014	1.018	1.008	1.008	1.008	1.010
Angle variance	61.7	62.4	55.7	58.6	74.1	31.3	33.8	30.9	41.8
Al octahedron									
Volume	8.93	8.76	8.58	8.69	8.59	9.56	9.42	9.40	8.62
Quadratic elongation	1.001	1.001	1.001	1.001	1.003	1.001	1.000	1.000	1.000
Angle variance	4.96	4.04	5.23	4.57	9.34	2.17	0.85	1.45	2.38
Eight-coordinated site									
Volume	20.12	19.96	19.71	19.59	19.16	23.9	23.3	23.2	23.4

shape; the aluminum octahedron changes size significantly more than the tetrahedron, but the octahedron remains regular; the eight-coordinated magnesium site shows the greatest variation with changes in temperature or pressure, and Mg-polyhedral expansion and compression coefficients are 50 percent larger than those of the aluminum octahedron.

Pyrope deviates from the inverse relationship in several important structural details. Unit-cell volume changes from 23°C to 750°C, and from 1 bar to 30 kbar, are both observed to be approximately 2 percent. The inverse relationship would suggest that the magnitudes of structural changes at 750°C would be comparable to those at 30 kbar. The silicon tetrahedron of pyrope, however, shows no change in size or shape between room temperature and 750°C, but does display a small compression at 30 kbar. Furthermore, in the eight-coordinated site the four longer bonds compress more than the four shorter Mg–O bonds, but the longer bonds expand *less* than the shorter bonds with increased temperature. It appears, therefore, that the inverse relationship applies to the general features of pyrope expansion and compression, but that the details of the response of garnet to temperature compared with pressure are different.

The inverse relationship is not expected to apply to minerals in which the ratio of mean polyhedral expansion $(\bar{\alpha})$ to mean polyhedral compression $(\bar{\beta})$ is very different for two polyhedra in the same mineral. Relative changes of polyhedral volumes on cooling *vs.* compression must be different, by definition, if $\bar{\alpha}/\bar{\beta}$ are different. In pyrope, $\bar{\alpha}/\bar{\beta}$ for the aluminum octahedron and that for the magnesium eight-coordinated site are both approximately 0.045 kbar/°C (observed); therefore, the inverse relationship holds. In grossular, however, both predicted and observed values of $\bar{\alpha}/\bar{\beta}$ for the aluminum octahedron are twice as large as for the calcium polyhedron. The aluminum octahedron in grossular, consequently, changes more with respect to the calcium site during cooling than during compression.

Hazen (1977) noted that temperature, pressure, and composition may be structurally analogous variables; in some structures, changes in temperature, pressure, or composition cause similar changes in atomic arrangements. In garnets of the form $R_3^{2+}Al_2Si_3O_{12}$, however, this analogy is valid only in the sense that changes in all three variables are accompanied by changes in the relative sizes of the three polyhedra. As demonstrated by Meagher (1975) for temperature and composition, and by this study for pressure, the garnet structure responds differently to changes in temperature, pressure, and composition.

Conclusions

The present investigation represents the most accurate high-pressure study of the crystal structure of a silicate to date. The average errors in bond distances are reduced from ±0.015A (Hazen and Burnham, 1975; Hazen, 1976b) to ±0.004A, and as a result detailed analysis of changes in polyhedral sizes and shapes with changes in pressure are possible. Two general conclusions regarding the response of garnet to pressure are:

(1) larger polyhedra with cations of lower charge are more compressible than smaller polyhedra with cations of higher charge; and,

(2) distorted polyhedra tend to become more regular at high pressure.

Both conclusions agree with observations made on gillespite (Hazen and Burnham, 1975) and olivine (Hazen, 1976b), and they are being further tested by experiments in progress on clinopyroxenes, silicate spinels, and oxides.

One of the objectives of this investigation was to test the empirical compression model of Hazen and Prewitt (1977). Although the relative values of polyhedral compressibilities were correctly predicted (*i.e.*, $\beta_{Si} < \beta_{Al} < \beta_{Mg} < \beta_{Ca}$), the absolute values of the predicted compressibilities were significantly lower than observed. It is concluded, therefore, that the Hazen and Prewitt compression equation, which is based primarily on $R^{2+}O$-type simple oxide compressibilities, must be modified as additional high-pressure structural refinements become available. Until such modifications are made, the empirical equation should be used primarily as a qualitative rather than a quantitative tool for predicting the variation of mineral structures with pressure.

References

Anderson, O. L., E. Schreiber, R. C. Liebermann and N. Soga (1968) Some elastic constant data on minerals relevant to geophysics. *Rev. Geophys., 6,* 491–524.

Bonczar, L. J., E. K. Graham and H. Wang (1977) The pressure and temperature dependence of the elastic constants of pyrope garnet. *J. Geophys. Res., 82,* 2529–2534.

Cromer, D. T. and D. Liberman (1970) Relativistic calculations of anomalous scattering factors for X-rays. *J. Chem. Phys., 53,* 1891–1898.

—— and J. B. Mann (1968) X-ray scattering factors computed

from numerical Hartree-Fock wave functions. *Acta Crystallogr., A24*, 321–324.

Finger, L. W. and R. M. Hazen (1977a) High-pressure crystal structures of the spinel polymorphs of Fe_2SiO_4 and Ni_2SiO_4. *Carnegie Inst. Wash. Year Book, 76*, 504–505.

—— and —— (1977b) Crystal structure and compressibility of ruby to 80 kbar. *Carnegie Inst. Wash. Year Book, 76*, 525–527.

—— and H. King (1978) A revised method of operation of the single-crystal diamond cell and the refinement of the structure of NaCl at 32 kbar. *Am. Mineral., 63*, 337–342.

—— and E. Prince (1975) A system of Fortran IV computer programs for crystal structure computations. *Natl. Bur. Stand. (U.S.) Tech. Note 854.*

——, C. G. Hadidiacos and Y. Ohashi (1973) A computer-automated, single-crystal X-ray diffractometer. *Carnegie Inst. Wash. Year Book, 72*, 694–699.

Gibbs, G. V. and J. V. Smith (1965) Refinement of the crystal structure of synthetic pyrope. *Am. Mineral., 50*, 2023–2039.

Graham, E. K. and T. J. Ahrens (1973) Shock wave compression of iron–silicate garnet. *J. Geophys. Res., 78*, 375–392.

Hamilton, W. C. (1965) Significance tests on the crystallographic *R* factor. *Acta Crystallogr., 18*, 502–510.

Hazen, R. M. (1976a) Effects of temperature and pressure on the cell dimension and X-ray temperature factors of periclase. *Am. Mineral., 61*, 266–271.

—— (1976b) Effects of temperature and pressure on the crystal structure of forsterite. *Am. Mineral., 61*, 1280–1293.

—— (1977) Temperature, pressure and composition: structurally analogous variables. *Phys. Chem. Minerals, 1*, 83–94.

—— and C. W. Burnham (1975) Crystal structure of gillespite II at 26 kbar: correction and addendum. *Am. Mineral., 60*, 937–938.

—— and C. T. Prewitt (1977) Effects of temperature and pressure on interatomic distances in oxygen-based minerals. *Am. Mineral., 62*, 309–315.

Huggins, F. (1974) *Mössbauer Studies of Iron Minerals under Pressures up to 200 kbar.* Ph. D. Thesis, Massachusetts Institute of Technology.

Meagher, E. P. (1975) The crystal structures of pyrope and grossularite at elevated temperatures. *Am. Mineral., 60*, 218–228.

Merrill, L. and W. Bassett (1974) Miniature diamond anvil pressure cell for single crystal X-ray diffraction studies. *Rev. Sci. Instrum., 45*, 290–294.

Piermarini, G. J., S. Block, J. D. Barnett and R. A. Forman (1975) Calibration of the pressure dependence of the R_1 ruby fluorescence line to 195 kbar. *J. Appl. Phys., 46*, 2774–2780.

Robinson, K., G. V. Gibbs and P. H. Ribbe (1971) Quadratic elongation: a quantitative measure of distortion in coordination polyhedra. *Science, 172*, 567–570.

Vaidya, S. N., S. Bailey, T. Pasternack and G. C. Kennedy (1973) Compressibility of fifteen minerals to 45 kilobars. *J. Geophys. Res., 78*, 6893–6898.

Verma, R. K. (1960) Elasticity of some high-density crystals. *J. Geophys. Res., 65*, 757–766.

Yoder, H. S., Jr. (1950) Stability relations of grossularite. *J. Geol., 58*, 221–253.